AJLISI
GLOBAL RESEARCH NETWORK

Information Horizons: AMERICAN Journal of Library And Information Science Innovation
Volume 4, Issue 01, 2026 ISSN (E): 2993-2777

Synthesis, Characterization, DFT and Molecular Docking Studies of Some New Imidazole Derivatives as Diabetes Drugs

Mohammed Ali Shnjar, Prof. Dr. Mahmood Shakir Magtoof
University of Thi-Qar, College of Science, Department of Chemistry, Thi-Qar, Nasiriyah 64001, Iraq

Abstract. *Researchers in the field of medicinal chemistry have focused their efforts on developing safer and less toxic pharmaceutical compounds for treating type 2 diabetes, compounds that can be used long-term without causing serious side effects. This study focused on the synthesis of two new imidazole derivatives using an alkaline medium and DMSO as a solvent. Good yields were obtained, and the chemical structure of the synthesized compounds was confirmed using infrared (IR) spectroscopy and proton-carbon nuclear magnetic resonance spectroscopy (1H NMR and 13C NMR). The results showed complete agreement with the theoretically predicted structures. In addition, two theoretical studies were conducted on the synthesized compounds, including density functional theory (DFT) calculations and molecular docking studies of the SIRT1 and GSK3β proteins. The results of these studies were then correlated with the analysis of the theoretical data. The results showed that compound 3β was the most effective of the synthesized compounds.*

Keywords: *Type 2 diabetes, imidazole derivatives, density functional theory, molecular docking.*

1. Introduction

Diabetes mellitus (DM) is classified as a chronic metabolic disease characterized by persistently high blood glucose levels. According to the International Diabetes Federation (IDF), approximately 537 million adults worldwide have been diagnosed with diabetes, and this number is expected to rise to 783 million by 2045[1, 2]. The seriousness of the disease lies in its chronic complications, which damage vital organs and blood vessels[3], including the eyes[4], kidneys[5], heart, and nervous system[6]. Diabetes is divided into two main types: Type 1 DM (T1DM), which results from insufficient or absent insulin secretion from the pancreas, and Type 2 DM (T2DM), which is associated with insulin resistance and decreased cellular responsiveness to insulin[7]. Type 2 DM is the most common form, accounting for approximately 80–90% of all cases worldwide[8, 9].

Imidazole, a fundamental heterocyclic compound with the molecular formula $C_3H_4N_2$, has emerged as one of the most versatile scaffolds in medicinal chemistry and drug development[10]. The imidazole ring system, consisting of a five-membered heterocycle with two nitrogen atoms at positions 1 and 3, occurs naturally in essential biomolecules including the amino acid histidine and the hormone histamine Figure 1. Its presence in these vital biological compounds underscores its significance in various physiological processes[11, 12].

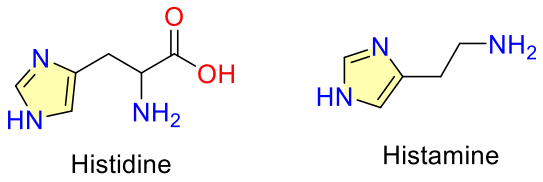

Figure 1 amino acid histidine and the hormone histamine

The remarkable characteristics of imidazole Figure 2 stem from its unique electronic structure and amphoteric nature[13]. The imidazole ring contains six π-electrons delocalized over five atoms, contributing to its aromatic character[14]. One nitrogen atom (N-1) is of the pyrrole type, while the other (N-3) resembles pyridine, allowing the molecule to act as both a base and a weak acid[15]. This dual nature enables imidazole derivatives to participate in various biochemical processes and interact effectively with different biological targets[16].

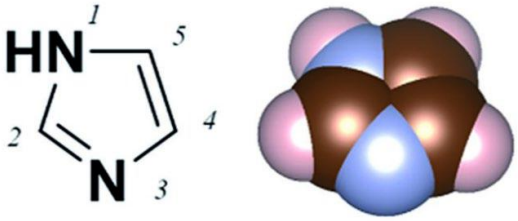

Figure 1 imidazole

Sirtuin 1 (SIRT1), a NAD+-dependent deacetylated protein enzyme, plays a pivotal role in regulating carbohydrate and lipid metabolism, improving insulin sensitivity, controlling inflammation, reducing oxidative stress, and maintaining mitochondrial integrity and function[17]. SIRT1 also contributes to the regulation of insulin secretion from pancreatic beta cells and protects them from damage caused by inflammation or oxidative stress[18]. Accordingly, several recent studies have focused on evaluating the efficacy of targeting SIRT1 as an innovative therapeutic approach for managing type 2 diabetes and reducing its complications.

Glycogen synthase kinase-3β (GSK-3β) is a key regulatory component of the insulin signaling pathway and plays a dual role in the pathogenesis of both type 2 diabetes and Alzheimer's disease. Under normal physiological conditions, insulin binding to its receptor triggers a cellular signaling cascade that activates protein kinase B (PKB/AKT), which in turn phosphorylates GSK-3β at Ser9, inactivating it[19]. This process contributes to enhanced glycogen synthesis and regulation of blood glucose levels. In type 2 diabetes, the insulin signaling pathway is impaired, leading to hyperactivation of GSK-3β[20].

In this study, two imidazole derivatives were synthesized. The aim was to examine the electronic and structural properties of the compounds using density functional theory. Furthermore, the molecular docking of these compounds to two important proteins, GSK-3β and SIRT1, was studied to explore their potential in developing them as future treatments for diabetes.

2. Materials and methods

2.1. Chemistry

All materials were used directly without the need for purification because they are of high purity and are required by reputable international companies in the field of chemicals.

2.1.1. General procedure for the synthesis of 1,2-bis((1H-imidazol-1-yl)methyl)benzene derivatives (6a-b)

Imidazole derivatives 4 (14.7 mmol) was dissolved in 12.5 ml of DMSO, and KOH (28.9 mmol, 1.6 g) was added. After 30 minutes of stirring, α,α'-dichloro-o-xylene 5 (7.25 mmol, 1.27 g) was added and the mixture was refluxed for 8 hours. The refluxed product was added to 300 ml of water. After

24 hours, N-alkylated 6(a-b) product was recovered.[21]

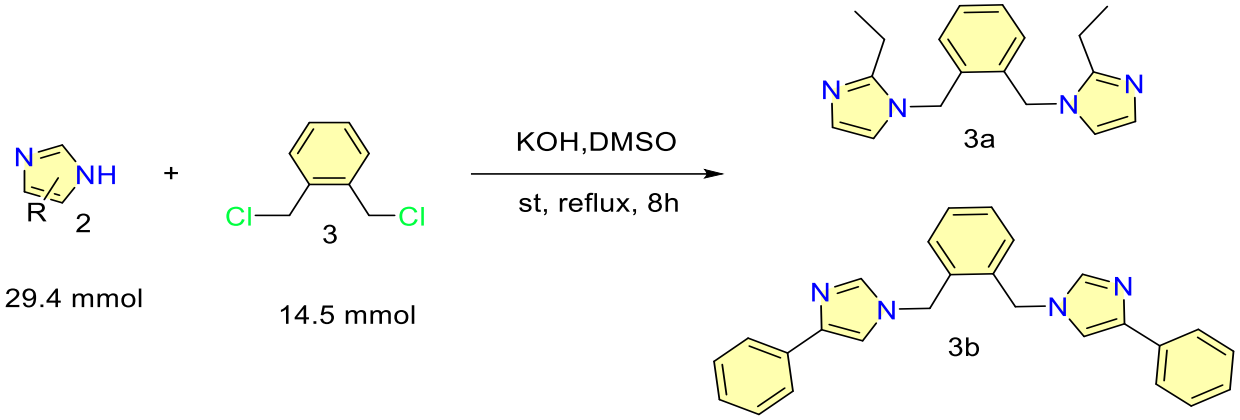

Scheme 1 synthesis of compound (3a-b)

Scheme2- 2 synthesis of compound (6a-b)

1,2-bis((2-ethyl-1H-imidazol-1-yl)methyl)benzene(3a)

Brown powder; yield: 62.2%; m.p.: 137-138°C ; Rf=0.47 (5 chloroform:5 ethanol) ; FT-IR 3127.7, 3106.49C-H(Ar), 2971.93, 2937.04, 2877.16(C-HAliph), 1691.88, 1660.43(C=N), 1523.37(C=C), 1433.4(C-N), (Cm-1);1H NMR (400 MHz, DMSO-d6) δ 7.24 (m, J = 5.8, 3.6 Hz, 1H), 7.03 (s, 1H), 6.89 (s, 1H), 6.53 (m, J = 5.5, 3.5 Hz, 1H), 5.27 (s, 2H), 2.52 (q, J = 7.4 Hz, 2H), 1.13 (t, J = 7.5 Hz, 3H)ppm. 13C NMR (101 MHz, DMSO) δ 12.48(CH3), 19.76(CH2), 46.07 (C-C-N), 120-136(Ar), 149.38 (C=N) ppm.

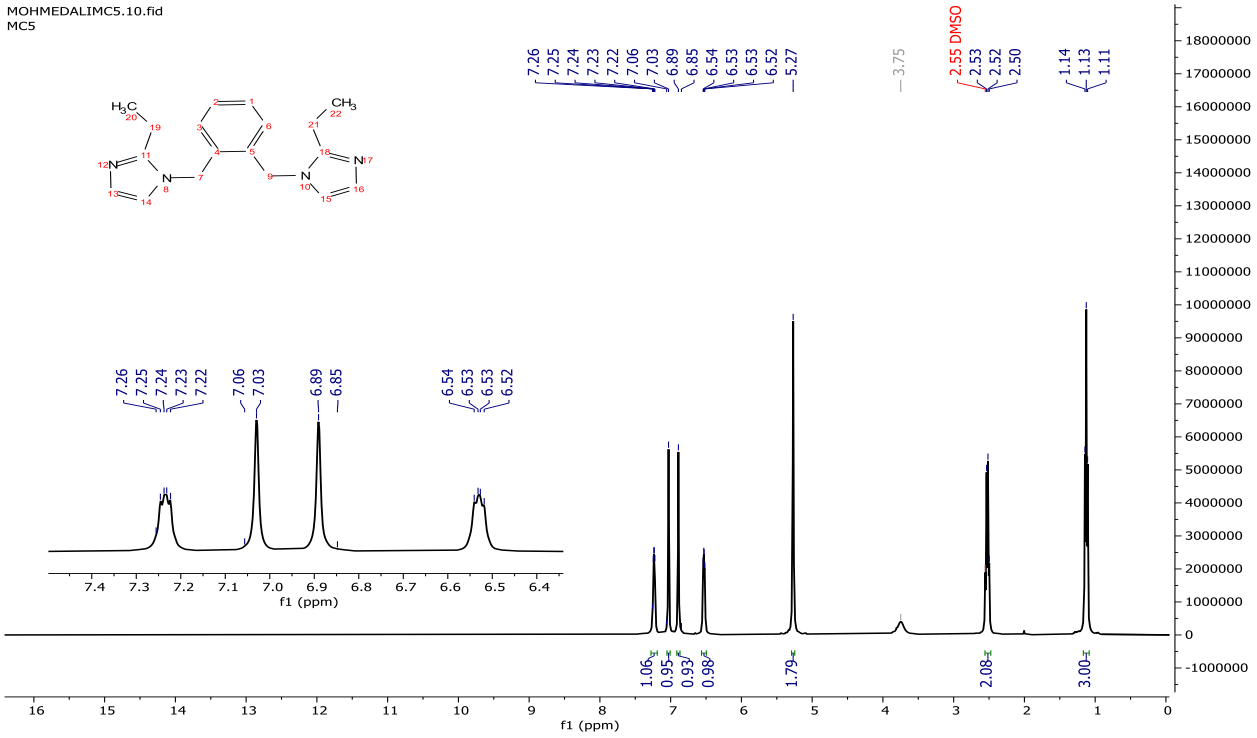

Figure 2 [1]HNMR spectrum of 3a

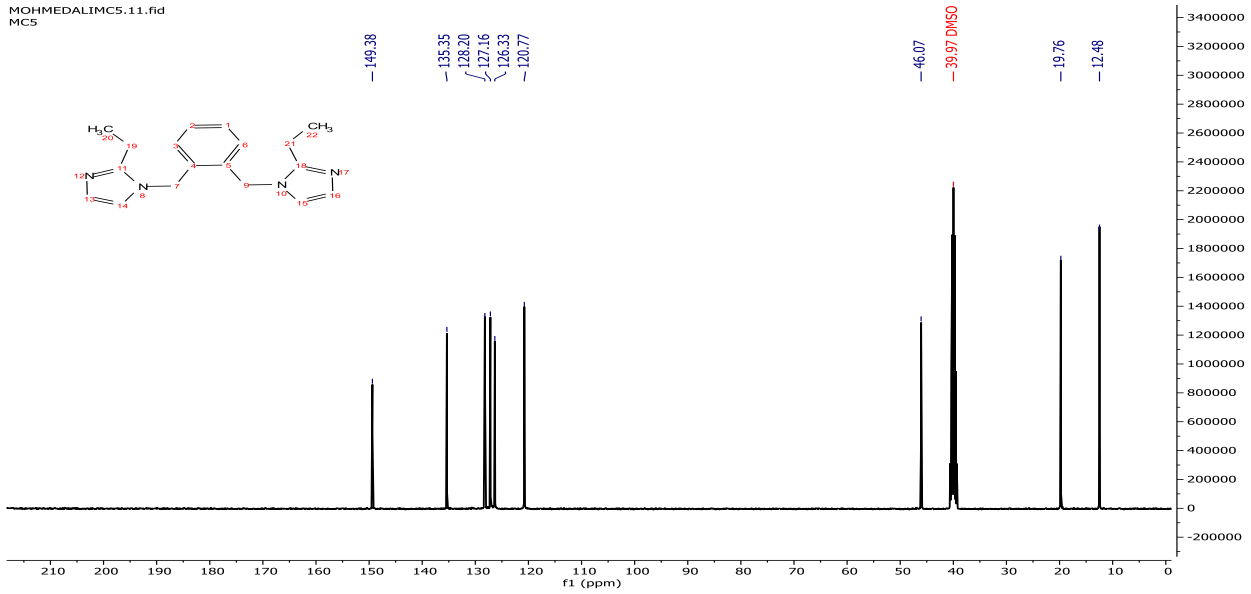

Figure 3 [13]CNMR spectrum of 3a

1,2-bis((4-phenyl-1H-imidazol-1-yl)methyl)benzene(3b)

Brown powder; yield: 65% ; m.p.: 148-149°C ; Rf=0.56 (5 chloroform:5 ethanol) ; FT-IR 3132.77, 3094.92, 3045.3, 3027.66, 3006.79 (C-H Ar), 2987.58, 2969.84, 2913.52, 2879.96, 283453(C-H Aliph), 1656.72(C=N), 1556.32(C=C), 1450(C-N) (Cm-1);1H NMR (400 MHz, DMSO-d6) δ 7.89 (d, J = 1.3 Hz, 1H), 7.79 – 7.72 (m, 2H), 7.46 (d, J = 1.3 Hz, 1H), 7.40 – 7.27 (m, 3H), 7.18 (td, J = 6.4, 2.6 Hz, 2H), 5.42 (s, 2H) ppm.

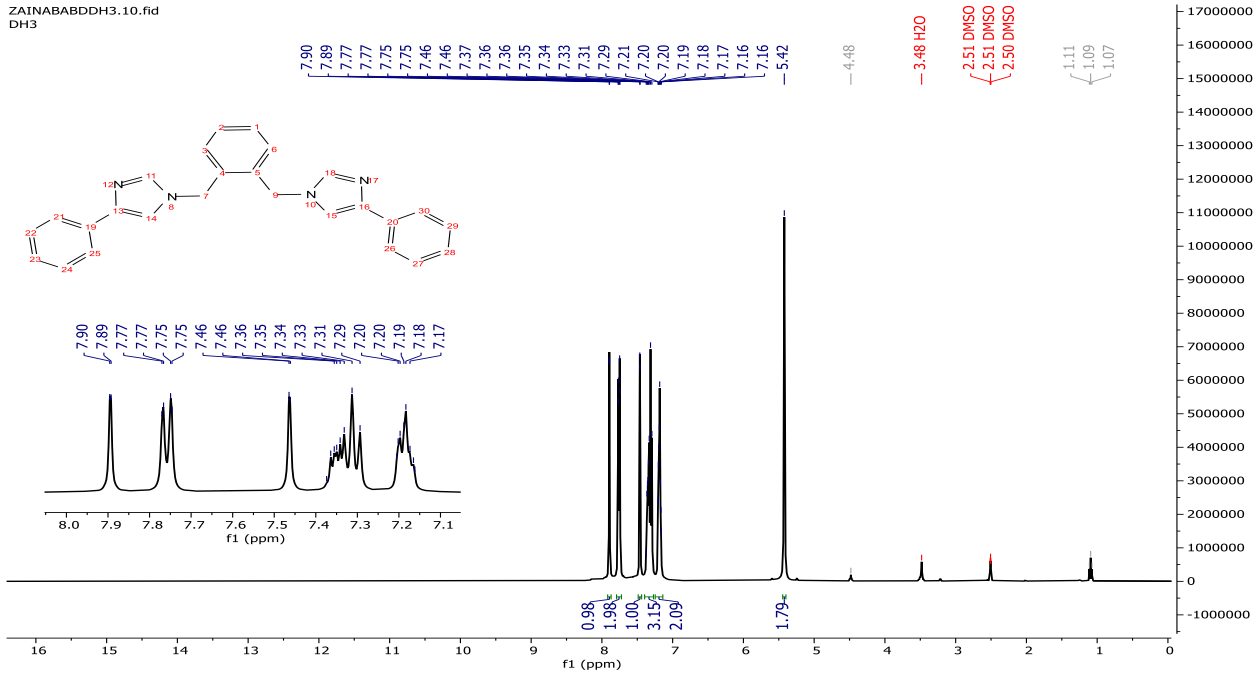

Figure 4 [1]HNMR spectrum of 3b

2.2. Density Functional Theory

Quantum chemical calculations were performed to investigate the structural and electronic properties of the compounds under study in the gas phase. All calculations were performed using density functional theory (DFT) using the B3LYP hybrid functional, which combines a three-parameter Becke exchange function and a Li-Yang-Barr correlation function. This level of theory is considered one of the most reliable due to its ability to achieve a reliable balance between computational efficiency and accuracy in characterizing organic compounds[22].

Geometric optimizations were performed using the 6-31G basis sets as implemented in the Gaussian 09 software[23], without imposing any symmetry constraints.

Front molecular orbital (FMO) analysis was also performed to determine the energy distribution of the highest occupied molecular orbital (HOMO) and lowest unoccupied molecular orbital (LUMO). The energy gap between the orbitals (ΔE = ELUMO – EHOMO) was also calculated, as it provides an important indicator of the chemical stability and charge transfer potential of the studied molecules[24].

E_g= ELUMO−EHOMO	(Energy band gap)	(1)
I.P= − EHOMO	(Ionization potential)	(2)
E.A= − ELUMO	(Electron affinity)	(3)
$\eta=\frac{(ELUMO-EHOMO)}{2}$	(Chemical hardness)	(4)
$\delta=\frac{1}{2\eta}$	(Chemical softness)	(5)
$\mu=\frac{(EHOMO+ELUMO)}{2}$	(Chemical potential)	(6)
$\omega=\frac{\mu 2}{2\eta}$	(electrophilicity)	(7)

Furthermore, global reactivity descriptors were evaluated using the Koopman approximation, based on well-known mathematical relationships based on the energy values of the frontier orbitals (EHOMO and ELUMO). These descriptors provide insights into the electron-donating and accepting properties, as well as the stability and chemical reactivity indicators of the studied compounds[25].

2.3. Molecular Docking

Molecular docking simulations were performed to study the binding interactions between the prepared compounds and the selected target proteins. The docking procedures were implemented using the Molecular Operating Environment (MOE, 2015) [26], a leading integrated platform for structure-based drug design.

Prior to docking, all molecules underwent energy minimization using the MMFF94x force field integrated into the MOE software to remove any potential structural stress. Partial charges were accurately calculated, and hydrogen atoms were added when necessary to ensure correct protonation at a physiological pH of 7.4.

The crystal structures of the target proteins were obtained from the Protein Data Bank (PDB) using the identifiers 5BTR and 1Q4L, for SIRT1 and GSK-3β, respectively[27, 28]. The proteins were prepared in MOE environment by removing water molecules within 4 Å of the binding site. The active site was identified based on the co-crystallized ligand and previously reported binding pocket residues.

Table2- 1 Binding sites residues used as input for receptor grid generation during Induced Fit Docking

Receptors	Site	Residues
SIRT1	1	1:(ASN155 LEU202 LYS203 LEU205 LEU206 PRO207 GLU208 THR209 ILE210 PRO211 PRO212 PRO213 GLU214 LEU215 THR219 GLN222 ILE223 ASN226 ILE227 LEU228 SER229 GLU230 PRO231 PRO232 LYS233 GLY261 ALA262 GLY263 SER265 VAL266 ILE270 PRO271 ASP272 PHE273 ARG274 SER275 PRO291 ASP292 GLN294 ALA295 PHE297 ASP298 ILE299 GLU300 TYR301 LYS304 GLN345 ASN346 ILE347 ASP348 ... IS471 LEU472 GLY480 ASP481 CYS482 ASP483)
GSK-3β	1	1:(SER66 PHE67 LYS85 VAL87 LEU88 GLN89 ASP90 PHE93 LYS94 ASN95 ARG96 GLU97 LEU128 LEU130 ARG180 PHE201 GLY202 SER203 ALA204)

3. Results and Discussion

3.1. Chemistry

3.1.1 Synthesis

Researchers continue to prepare and discover numerous new pharmaceutical compounds for use as treatments for diabetes, despite the availability of many proven therapies. In this study, two new imidazole derivatives were synthesized by combining imidazole derivatives with α, α-dichlororthoxylene in a basic KOH medium using DMSO as a solvent. The resulting product showed a relatively good yield of 62.2-65%.

3.1.2. Characterization

The synthesized compounds exhibited spectra consistent with their predicted structural design. FTIR spectroscopy was performed, yielding the expected bands for the functional groups, as shown in Table 2.

Table 2 FT-IR band of 3a-3b

Comp.	C-H(Ar)	C-H(Aliph)	C=N	C=C	C-N
3a	3127.7 3106.49	2971.93 2937.04 2877.16	1691.88 1660.43	1523.37	1433.4
3b	3132.77 3094.92 3045.3 3027.66 3006.79	2987.58 2969.84 2913.52 2879.96 283453	1656.72	1556.32	1450

Furthermore, Figures 3,5 shows the ^{1}HNMR spectra of the synthetic compounds, indicating their purity and the appearance of their expected shifts. Finally, Figure 4 shows the ^{13}CNMR spectrum of synthetic compound 3a, showing the chemical shifts consistent with the structural composition of the synthetic compound.

3.2. Density Functional Theory (DFT)

Figure C shows the improved molecular structures of the synthetic compounds 3a to 3b, obtained through DFT calculations show in figure 6. These structures reveal the stability, reactivity, and chemical behavior of the molecules, as shown in Table 3. The high values of the energy level of the higher molecular orbitals occupied by electrons HOMO indicate that the molecule behaves as a π-donor, while the opposite is true for LUMO, where the molecule behaves as a π-acceptor[29].

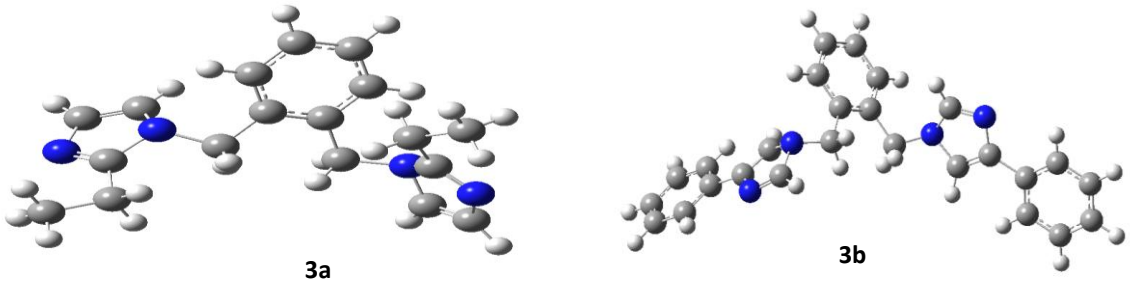

Figure 5 The Optimized geometrical structures of synthetic compounds 3a-b

In this context, compound 3A exhibited a lower HOMO value of -0.2291 than compound 3B, indicating that compound 3A is more stable and less reactive, while compound 3B is less stable and more reactive. Regarding the LUMO value, the energy values for compound 3a were -0.0177 and 3b -0.0281, reflecting 3b ability to accept electrons, as its LUMO value is lower than that of compound 3a. These results are consistent with molecular orbital theory, which posits that molecules with low HOMO and LUMO values exhibit greater stability and lower reactivity[30].

Table 3 . Electronic parameters for the investigated systems computed 3a-b at B3LYP /6-31G

comp	HOMO	LUMO	di	E gap	IP	EA	η	δ	μ	ω
3a	-0.2291	-0.0177	1.0289	5.7543	0.2291	0.0177	2.8771	0.1737	-3.3590	1.9608
3b	-0.2201	-0.0281	1.2704	5.2242	0.2201	0.0281	2.6121	0.1914	-3.3770	2.1829

EH: HOMO energy (**eV**), **EL**: LUMO energy (**eV**), **Egap**: Energy gap (**eV**), **η**: Chemical hardness (**eV**), **δ**: Chemical softness (**eV^{-1}**), **μ**; Chemical potential (**eV**), **ω**; Electrophilicity (**eV**).

The difference between the higher energy level (HOMO) and the lower energy level (LOMO) is known as the energy gap, which is an important indicator of chemical activity. The lower the Egap value, the more active the compound, and the higher the gap value, the less active the compound. Therefore, the gap value for compound 3b (5.2242) is lower than that of 3a (5.7543), making 3b more active than 3a.

Furthermore, in this study, we performed calculations for chemical hardness and ductility. Compound 3a had a hardness value of 2.8771 and a ductility value of 0.1737, indicating its high stability and low activity. Conversely, compound 3b had a hardness value of 2.6121 and a softness value of 0.1914, making it less stable and more reactive. Pearson's principle for shock and soft acids and bases (HSAB) states that harder compounds are more stable and less reactive [31].

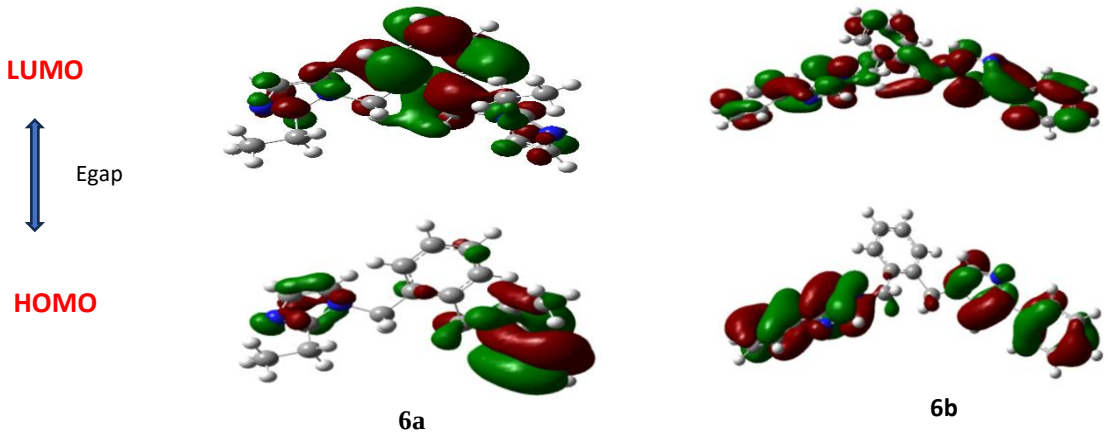

Figure 6 The HOMO and LUMO orbitals of Synthetic compounds 3a-3b

We also calculated the polar properties of the synthesized compounds. The dipole moment of compound 3b (1.2704) was higher than that of compound 3a (1.0289). This indicates that compound 3b has a higher polarity and a greater capacity for forming intense intermolecular interactions. These results confirm the pivotal role of the dipole moment in determining the strength of molecular interactions, which in turn influences the physical and chemical properties of compounds[32].

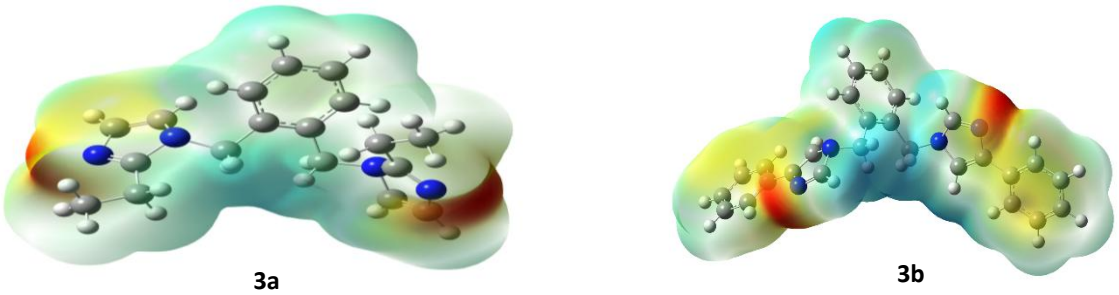

Figure 7 MEP Maps of Synthetic compounds 3a-3b

Furthermore, compound 3a exhibited the lowest chemical potential (1.9608) and the highest electronegativity. This makes it thermally stable because its electrons are strongly bonded in low energy levels. These results are consistent with the concept that molecules with higher (ω) values are typically more reactive and less stable[33].

3.3. Molecular Docking

3.3.1. Binding Affinity of Compounds to the Active Site of SIRT1

Table 4 and figure 9 shows that compound 3a has a binding energy of -5.8151 and an RMSD value of 1.8147. This is considered a good value, close to 2. Furthermore, it formed three strong bonds with the protein pocket 1. The N44 of the compound bonded to the NZ of the amino acid LYS233 via an H-acceptor hydrogen bond, 3.6 away, with an energy of -0.5. The second bond of compound 3a was a 6-ring bond with CD2 of the amino acid LEU206 via a pi-H bond. The third bond was a 5-ring bond with the amino acid HIS471 via a pi-pi bond.

Table 4 The results obtained from docking of Synthetic compounds 3a-3b with SIRT1 in site 1.

compound	S score (kcal/mol)	RMSD (Å)	Atom of compound	Atom of receptor	Involved receptor residues	Type of interaction bond	Distance (Å)	E (kcal/mol)
3a	-5.8151	1.8147	N 44	NZ	LYS 233	H-acceptor	3.61	-0.5
			6-ring	CD2	LEU 206	pi-H	4.06	-0.5
			5-ring	5-ring	HIS 471	pi-pi	3.91	
3b	-7.6070	1.6327	5-ring	CB	LYS 444	pi-H	3.84	-1.2
			5-ring	5-ring	HIS 471	pi-pi	4.07	

Additionally, the compound gave synth 3b an excellent binding energy of -7.6070 and an acceptable RMSD value of 1.6327. The binding occurred at two sites: 2×5-ring bonds with CB and 5-ring bonds of the amino acids LYS444 and HIS471, via pi-H and pi-pi bonds with a distance of 3.84 and 4.07, and a good energy of -1.2, respectively.

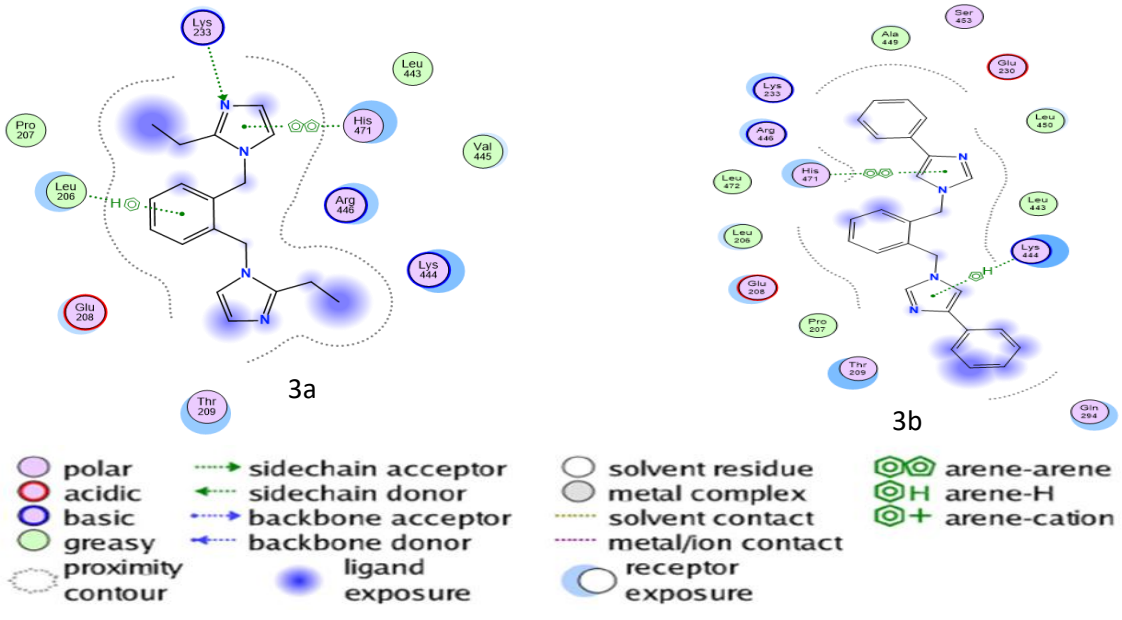

Figure 8 Ligand binding interactions in the active site 1 of SIRT1

3.3.2. Binding Affinity of Compounds to the Active Site of GSK-3β

Table 5 and figure 10 shows that compound 3a has a binding energy to the amino acid residues of the protein GSK3B -6.3590 and an RMSD value of 1.6058. Furthermore, it formed three pi-H bonds through the components of the synthetic compound C11, 5-ring and 6-ring bonds with 6-ring, NE2 and ND2 bonds with the amino acid residues PHE 67, GLN 89 and ASN 95, respectively.

Table 5 The results obtained from docking of Synthetic compounds 3a-3b with GSK-3β in site 1.

compound	S score (kcal/mol)	RMSD (Å)	Atom of compound	Atom of receptor	Involved receptor residues	Type of interaction bond	Distance (Å)	E (kcal/mol)
3a	-6.3590	1.6058	C 11	6-ring	PHE 67	H-pi	4.20	-0.5
			5-ring	NE2	GLN 89	pi-H	4.81	-0.6
			6-ring	ND2	ASN 95	pi-H	4.42	-0.5
3b	-6.2345	2.6149	6-ring	CB	LEU 88	pi-H	4.03	-0.5
			5-ring	CB	ASP 90	pi-H	3.78	-0.5
			5-ring	CA	ASN 95	pi-H	4.15	-1.0
			5-ring	N	ARG 96	pi-H	3.65	-1.6

Furthermore, the 3b compound showed associations with the amino acid residues of the aforementioned protein, also of the pi-H type, through the components of the 6-ring and 3x5-ring compound with the CB, CB, CA and N of amino acid LEU88, ASP90, ASN95 and ARG96, respectively.

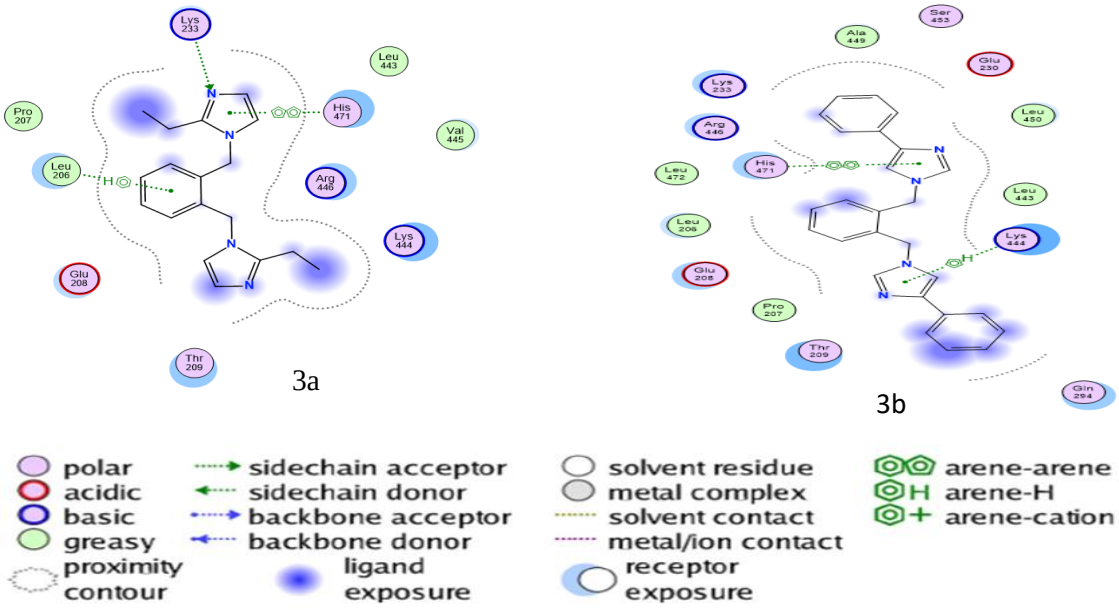

Figure 9 Ligand binding interactions in the active site 1 of GSK-3β

3.4. Combining Molecular Docking Results with Density Functional Theory (DFT)

Based on the aforementioned results concerning compounds 3a and 3b, compound 3b exhibited lower stability and higher reactivity. This is attributed to its relatively low homo value (-0.2201) and its higher electron-accepting capacity (lumo value -0.0281). Furthermore, it had a lower eGa value of 5.2242 than 3a, a lower chemical hardness value of 2.6121, and a higher dipole moment of 1.2704, resulting in higher polarity and reactivity.

Additionally, it demonstrated excellent binding energy (-7.6070) with the SIRT1 protein. It also formed four pi-H bonds with good binding energy (-6.2345) with the GSK-3β protein. This makes compound 3b superior to compound 3a in terms of chemical and reactivity properties.

4. Conclusions

In summary, we synthesized and characterized two new organic compounds, designated 3a and 3b, using a basic reflux distillation method with the non-protonizing solvent dmso. The resulting derivatives were characterized using FTIR, 1H-NMR, and 13C-NMR spectroscopy. Compound 3b was the most promising in this study, exhibiting the best results in density functional theory (DFT) and molecular docking calculations. The study of the relationship between chemical structure and theoretical biological activity highlighted the importance of the electronic and structural properties of the synthesized compound 3b, such as its energy gap value and chemical stiffness, which form strong

bonds with the studied proteins in molecular docking, thus enhancing its anti-diabetic activity. The outstanding performance of compound 3b in treating diabetes warrants further investigation into its efficacy and safety, making it a promising candidate for the development of more effective and safer diabetes medications. These results offer valuable insights for future research efforts aimed at developing treatment options for diabetes.

Statement of Authors' Contributions:

Mohammad Ali Shanjar: Contributed to the conceptualization, methodology, research, formal analysis, and writing of the original manuscript.

Professor Dr. Mahmoud Shaker Majtouf: Assisted in data validation, processing, computational studies, writing, review, and editing. Specifically, Mohammad Ali Shengar conducted the synthesis and characterization experiments, while Professor Dr. Mahmoud Shaker Majtouf conducted the theoretical molecular docking against type 2 diabetes, the computational studies to determine the energy gap, and reviewed and approved the final manuscript.

References

1. K. Sharma, H. Ambawat, and N. Gupta, "A Comprehensive Review of Diabetes Mellitus: From Pathogenesis to Patient-Centered Team Care," *IJSAT-International Journal on Science and Technology*, vol. 16, no. 4, 2025.
2. A. A. Yameny, "Diabetes mellitus overview 2024," *Journal of Bioscience and Applied Research*, vol. 10, no. 3, pp. 641-645, 2024.
3. S. M. Jwad and A.-F. Hawraa Yousif, "The Effect of Diabetes on the Possessions of Blood and Vessels," *Journal of Advances in Pharmacy Practices*, vol. 4, no. 1, pp. 15-20, 2022.
4. A. Dubey and S. Lohiya, "Changes in eyes in a diabetic patient," *Journal of Pharmaceutical Research International*, vol. 33, no. 61A, pp. 480-485, 2021.
5. N. M. Abed, "Effect of vitamin D3 on liver and kidney function of diabetes mellitus male rats," *University of Thi-Qar Journal of Science*, vol. 7, no. 2, pp. 80-83, 2020.
6. L. O. Farhan and I. N. Salman, "A review on the role of novel adipokine Isthmin-1 and Subfatin in human type 2 diabetes mellitus," *University of Thi-Qar Journal of Science*, vol. 10, no. 2, pp. 181-186, 2023.
7. C. Solis-Herrera, C. Triplitt, C. Reasner, R. A. DeFronzo, and E. Cersosimo, "Classification of diabetes mellitus," *Endotext [Internet]*, 2018.
8. M. J. Hossain, M. Al-Mamun, and M. R. Islam, "Diabetes mellitus, the fastest growing global public health concern: Early detection should be focused," *Health Science Reports*, vol. 7, no. 3, p. e2004, 2024.
9. B. ahmed abed, L. Othman Farhan, I. Noori Salman, and s. ehssan, "A review on the role of novel adipokine Isthmin-1 and Subfatin in human type 2 diabetes mellitus," *University of Thi-Qar Journal of Science*, vol. 10, no. 2, pp. 181-186, 12/27 2023, doi: 10.32792/utq/utjsci/v10i2.1129.
10. L. Zhang, X. M. Peng, G. L. Damu, R. X. Geng, and C. H. Zhou, "Comprehensive review in current developments of imidazole-based medicinal chemistry," *Medicinal research reviews*, vol. 34, no. 2, pp. 340-437, 2014.
11. S. Katke, "Imidazole: Chemistry, Synthesis, Properties, Industrial Applications and Biological and Medicinal Applications," *Environmental Science. An Indian Journal*, vol. 19, no. 1, pp. 257-267, 2022.
12. A. A. Ali, "Synthesis and Spectrophotometric Study of Some New Azodyes Derived From 4,5-diphenylimidazole," *University of Thi-Qar Journal of Science*, vol. 4, no. 3, pp. 83-89, 06/05 2014, doi: 10.32792/utq/utjsci/v4i3.637.

13. M.-A. Codescu *et al.*, "Ultrafast proton transfer pathways mediated by amphoteric imidazole," *The Journal of Physical Chemistry Letters*, vol. 14, no. 20, pp. 4775-4785, 2023.

14. K. R. Sapkota, J. Begam, and S. Kumari, "A Novel Imidazole Derivative: Synthesis, Spectral Characterization, and DFT Study," *AMC Multidisciplinary Research Journal*, vol. 4, no. 1, pp. 79-88, 2025.

15. F. Edition, "Heterocyclic Chemistry."

16. A. Verma, S. Joshi, and D. Singh, "Imidazole: Having versatile biological activities," *Journal of Chemistry*, vol. 2013, no. 1, p. 329412, 2013.

17. H. Zhang *et al.*, "The Role of Hepatic SIRT1: From Metabolic Regulation to Immune Modulation and Multi-target Therapeutic Strategies," *Journal of Clinical and Translational Hepatology*, vol. 13, no. 10, p. 878, 2025.

18. G. Guan, Y. Chen, and Y. Dong, "Unraveling the AMPK-SIRT1-FOXO pathway: the in-depth analysis and breakthrough prospects of oxidative stress-induced diseases," *Antioxidants*, vol. 14, no. 1, p. 70, 2025.

19. H. Alhassan, K. Janiyani, M. Surti, M. Adnan, and M. Patel, "The Dual Role of Glycogen Synthase Kinase-3 Beta (GSK3β) in Neurodegenerative Pathologies: Interplay Between Autophagy Disease Progression," *Frontiers in Pharmacology*, vol. 16, p. 1693805, 2025.

20. B. RH, "The possible involvement of glycogen synthase kinase-3 (GSK-3) in diabetes, cancer and central nervous system diseases," *Current pharmaceutical design*, vol. 17, no. 22, pp. 2264-2277, 2011.

21. N. Naz, S. Saqib, R. Ashraf, M. I. Majeed, and M. A. Iqbal, "Synthesis of new organoselenium compounds: characterization and biological studies," *Macedonian Journal of Chemistry and Chemical Engineering*, vol. 39, no. 1, pp. 1-10, 2020.

22. S. Ismaeel, S. Bibi, S. Jamil, and M. Yaseen, "Improving small-molecules based OSCs performance through molecular optimization: a computational DFT analysis," *Journal of Fluorescence*, pp. 1-18, 2025.

23. M. Frisch *et al.*, "Gaussian 16 (Gaussian, Inc., Wallingford, CT, 2016)," *Wavelength/nm*, vol. 200, pp. 300-400, 2024.

24. M. Shuaibu, A. M. Ayuba, and B. Usman, "Computational Insights into the Corrosion Inhibition Potential of 9-Octadecenal on Mild Steel: A DFT and Molecular Dynamics Study," *Eurasian J. Sci. Technol*, vol. 5, no. 4, pp. 322-342, 2025.

25. A. M. Alsanafi and N. H. Al-Saadawy, "Synthesis, characterization, cyclic voltammetry (CV), theoretical molecular docking against breast cancer and computational study to determine the energy gap of a newly series of organotillium compounds based on N-(4-benzoylphenyl)–2–tellerocyanatoacetamide," *Trends in Sciences*, vol. 22, no. 9, pp. 10416-10416, 2025.

26. M. O. Environment, "Chemical Computing Group ULC., 1010 Sherbooke St. West, Suite# 910, Montreal, QC, Canada, H3A 2R7," 2022.02.

27. D. Cao, Wang, M., Qiu, X., Liu, D., Jiang, H., Yang, N., Xu, R.M., "Crystal structure of SIRT1 in complex with resveratrol and an AMC-containing peptide," ed. PDB, 2015-07-08.

28. J. A. Bertrand, Thieffine, S., Vulpetti, A., Cristiani, C., Valsasina, B., Knapp, S., Kalisz, H.M., Flocco, M., "GSK-3 Beta complexed with Inhibitor I-5," ed. PDB, 2003-10-14

29. S. Bedoura, H.-W. Xi, H. W. Goh, and K. H. Lim, "DFT/TDDFT Investigation on donor-acceptor triazole-based copolymers for organic photovoltaics," *Journal of Molecular Structure*, vol. 1248, p. 131406, 2022.

30. V. Choudhary, A. Bhatt, D. Dash, and N. Sharma, "DFT calculations on molecular structures, HOMO–LUMO study, reactivity descriptors and spectral analyses of newly synthesized

diorganotin (IV) 2-chloridophenylacetohydroxamate complexes," *Journal of computational chemistry*, vol. 40, no. 27, pp. 2354-2363, 2019.

31. F. F. Mulks, "Hard and soft electrons and holes," *Chem*, vol. 10, no. 9, pp. 2724-2744, 2024.
32. M. F. Khan, R. B. Rashid, M. M. Rahman, M. Al Faruk, M. M. Rahman, and M. A. Rashid, "Effects of solvent polarity on solvation free energy, dipole moment, polarizability, hyperpolarizability and molecular reactivity of aspirin," *Int. J. Pharm. Pharm. Sci*, vol. 9, no. 2, pp. 217-221, 2017.
33. N. Ree, J. M. Wollschläger, A. H. Göller, and J. H. Jensen, "Atom-based machine learning for estimating nucleophilicity and electrophilicity with applications to retrosynthesis and chemical stability," *Chemical Science*, vol. 16, no. 13, pp. 5676-5687, 2025.